



Using Guanidinium Groups for the Recognition of RNA and as Catalysts for the Hydrolysis of RNA

Denise M. Perreault, Larry A. Cabell and Eric V. Anslyn*

Department of Chemistry and Biochemistry, The University of Texas at Austin, Austin, TX 78712, U.S.A.

Abstract—The guanidinium functional group is commonly used in nature to recognize and bind anions through ion pairing and hydrogen bonding. Specific hydrogen-bonding patterns can be found in crystal structures of simple guanidinium salts. Analysis of these simple salts reveals a variety of features which are found in natural systems. These features have been applied to a series of artificial phosphodiesterases for RNA. These receptors incorporate guanidinium groups positioned to mimic the hydrogen-bonding patterns found in simple guanidinium salts and natural enzymes. This paper outlines general guanidinium hydrogen-bonding patterns. Next, the complexation of phosphodiesters with a series of artificial receptors are analyzed in terms of counterions, solvent mixtures, and cavity flexibility. In addition, strategies to enhance catalysis through a pK_a analysis of phosphoranes are addressed. Next, we describe how our findings were incorporated into second generation receptors/catalysts. Finally, our future work is discussed. © 1997 Elsevier Science Ltd.

Introduction

The guanidinium functional group is part of the side chain of the essential amino acid arginine. In contrast to the alcohol of serine, the carboxylate of glutamic acid, the amine of lysine, and other side chains, guanidinium is one of the more exotic functional groups in nature. It contains three amines in a plane, and it remains protonated over a wide pH range. It can form up to five hydrogen bonds when present within the arginine side chain. These structural features make it a versatile moiety for molecular recognition and catalysis. Herein, the roles that guanidinium groups play in recognition and catalysis are discussed with focus on RNA and DNA transformations.¹

The roles of guanidiniums in RNA recognition

Simple salts

Crystal structures of simple guanidinium derivatives reveal a variety of features that are found in natural systems. Several crystal structures of guanidinium groups with phosphates bound have been solved.² In general there are three different hydrogen-bonding arrangements from guanidiniums to phosphates. The most common motif involves two hydrogen bonds from the guanidinium to the phosphate, each from different

NHs to different oxygens (Fig. 1A). Two other patterns involving either an NH_2 bridging between two phosphate oxygens or different NHs bonding to the same oxygen are found less often (Fig. 1B and C, respectively).³ These three patterns are to be expected in the recognition of the phosphodiesters of RNA by arginine-containing proteins and enzymes. In fact, higher order aggregates found in biological recognition have also been found in simple salts.

As will be discussed below, staphylococcal nuclease (SNase) binds a phosphodiester with two guanidinium groups present at Arg-35 and Arg-87 using the two-point hydrogen-bonding pattern shown in Figure 1A. Not surprisingly, such a pattern is also found in simple salts. Figure 2 shows the hydrogen-bonding pattern in a crystal of bis(methylguanidinium) monohydrogen phosphate.⁴ The pattern is a set of two strong hydrogen bonds from each guanidinium to the phosphate. Another example of a simple salt mimicking a natural recognition motif is shown in Figure 3. One proposal of arginine recognition of phosphates in RNA is a motif called the ‘arginine fork’.⁵ In this motif, a single guanidinium bridges two phosphates in the RNA chain forming a total of four hydrogen bonds. This exact pattern was found in the crystal structure of methylguanidinium nitrate⁶ in 1955 and again in 1976 in the crystal structure of bis-guanidinium hydrogen phosphate.⁷ Thus, the hydrogen-bonding patterns found in simple

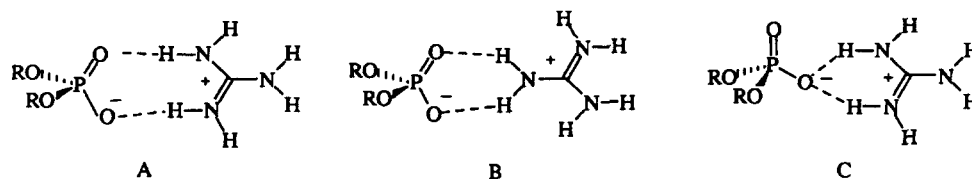


Figure 1. General hydrogen-bonding patterns from guanidiniums to phosphates.

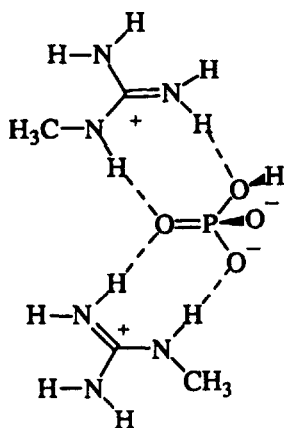


Figure 2. Hydrogen-bonding pattern in a crystal of bis(methylguanidinium) monohydrogen phosphate.

salts give considerable insight into those used in natural systems, and they can serve as a paradigm for those which nature is likely to use in the recognition of RNA.

Tat-TAR interactions

We first examine Tat-TAR interactions as an example of an RNA recognition motif that is found in simple salts. The HIV Tat protein interacts with TAR-RNA specifically at a hairpin located at the 5'-end of viral mRNA.⁸ This binding is essential for Tat to act as a transcriptional activator.⁹ There are two stem regions of TAR separated by three unpaired nucleotides in a bulge, while the loop consists of six nucleotides (Fig. 4). The loop is not involved in binding but is involved during transcriptional activation.

The binding of Tat to TAR involves a single essential arginine residue in a stretch of nine basic amino acids.⁵ Arginine itself can play the same role.¹⁰ The role of the guanidinium moiety in the recognition process has been studied extensively. One postulate was that the guanidinium group bridges two phosphates in an interaction referred to as the 'arginine fork' similar to that shown in Figure 3. The close proximity of two phosphates forms a space complementary to a guanidinium and this cavity should be present near RNA loops and bulges, not within double-stranded A-form RNA. The guanidinium thus interacts with these RNA geometries. This inter-

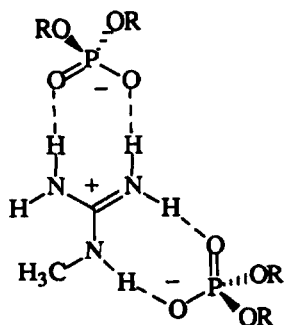


Figure 3. 'Arginine fork' motif in which a single guanidinium bridges two phosphates.

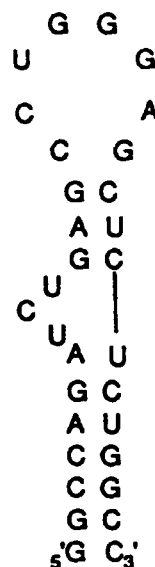


Figure 4. The sequence and secondary structure of TAR RNA.

action is a driving force for the protein-RNA bindings and could account for the RNA conformational change found for the binding of HIV Tat.¹¹

The original arginine fork idea has been modified slightly based on results from multidimensional NMR studies.¹² The new model contains many of the features of the original model, including the contact of one guanidinium group with two phosphodiester. The refinement of this model involves further interactions with a guanosine in the minor groove (Fig. 5). Therefore, the guanidinium makes three contacts when arginine or the nine amino acid sequence binds with TAR.

This well-characterized binding between an RNA molecule and a peptide is not the only example of such recognition. The unstacking of bases to form very specific structures between tRNAs and aminoacyl-tRNA synthetases has been observed.¹³ Most commonly, the protein-RNA interactions occur in single-

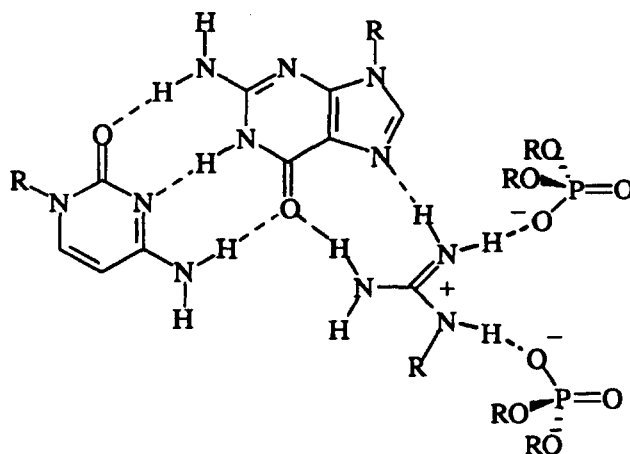


Figure 5. Hydrogen-bonding contacts of arginine with guanine and with two phosphates in TAR.

stranded regions or at the junction of single and double strands.¹⁴ Furthermore, crystal structures of DNA– and RNA–protein complexes reveal guanidinium interactions with nucleotide bases and phosphoester groups.¹⁵ As with the Tat–TAR interaction, guanidinium has been found to bind to the guanosine binding site in the *Tetrahymena* intron.¹⁶ In addition, the zinc-finger binding motif for DNA can involve a specific guanidinium–guanosine interaction along with guanidinium–aspartic acid recognition.¹⁷ All these examples highlight the utility and versatility of the guanidinium group for nucleotide recognition.

The roles of guanidinium in RNA and DNA hydrolysis

Staphylococcal nuclease

Staphylococcal nuclease is a DNA and RNA phosphodiesterase. The enzyme catalyzes the hydrolysis at the 5'-position of the phosphodiester. A Ca^{+2} is required for activity and cannot be replaced with other ions without a significant decrease in activity. The mechanism was first put forth after inspection of a 1.5 Å resolution crystal structure with pdTp bound (Fig. 6).¹⁸ Two guanidinium groups complex the phosphate. Arg-35 hydrogen bonds to the phosphomonoester as well as to the amide carboxyl oxygens of Leu-36 and Val-39, while Arg-87 binds to the phosphomonoester and a carboxyl group of Asp-83. The mechanism involves general base (Glu-43) assisted nucleophilic attack of water (possibly the 2'-OH in RNA) on the 5'-phosphate in line with the 5'-C-O-P bond. A trigonal bipyramidal phosphorane intermediate is formed. The ionic bond between the Ca^{+2} and the phosphate, as well as the four hydrogen bonds from the guanidinium groups, are postulated to stabilize the transition state and the formation of the dianionic phosphorane. The cation and the guanidinium groups act as Lewis acids and electrostatic catalysts; in addition, the guanidiniums may act as Brønsted acids. The expulsion of the leaving group may

require a proton transfer from a guanidinium. Thus the guanidinium groups are involved in both steps of the reaction: the nucleophilic attack and the leaving group departure.

The roles of the guanidiniums have been probed by Mildvan using single- and double-site-directed mutagenesis. When the arginines are changed to glycine, a mutation at Arg-35 results in very weak substrate binding, while the binding is affected only slightly by the same mutation at Arg-87.¹⁹ However, the mutation at Arg-87 has a dramatic effect on *k*_{cat}. Mildvan postulates that Arg-87 interacts only with the trigonal bipyramidal transition state rather than with the substrate.²⁰ The current interpretation is that Arg-87 forms a hydrogen bond to the apical leaving group of the phosphorane intermediate and acts as a general acid to assist leaving group departure. Altogether, the combination of the two guanidinium groups results in a greater than 10⁴-fold rate enhancement for hydrolysis.

Guanidiniums in artificial receptors and catalysts

Complexation

Our group has been examining artificial phosphodiesterases of RNA. These artificial enzymes incorporate guanidinium groups for the recognition of the phosphodiester linkages in RNA, as well as for electrophilic activation of the phosphodiester toward nucleophilic attack. A variety of receptors were analyzed for both binding and catalysis (Fig. 7). Receptors **3–11** possess aminoimidazoline groups as

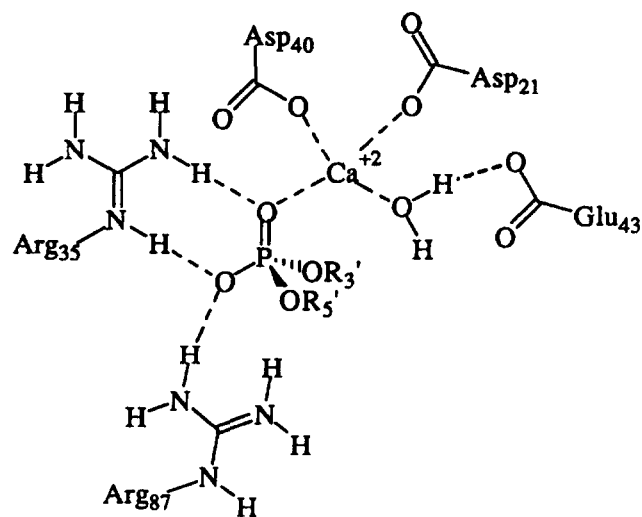


Figure 6. Schematic representation of the active site of SNase.

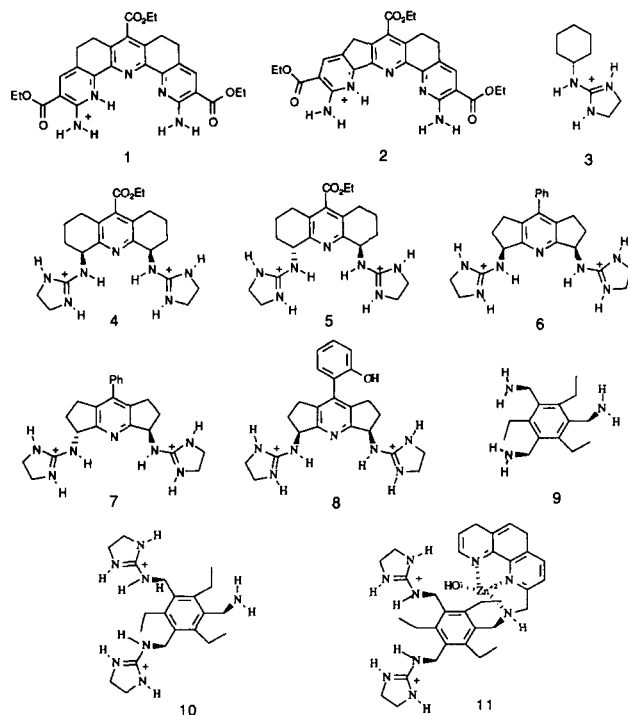


Figure 7. Artificial RNA phosphodiesterases.

mimics of guanidinium groups. The aminoimidazoline groups have the same two-point hydrogen bonding capabilities as guanidiniums, except that the hydrogen bonds are directed only toward the binding site. In addition, the aminoimidazoline groups have pK_a s similar to those of guanidiniums, so that they are protonated over a wide pH range. Furthermore, all these receptors are highly preorganized: either fused cyclic rings or alternating steric bulk was used to impart the preorganization of the functional groups. Preorganization is necessary for several reasons. First, the binding strength must be maximized by lowering the degrees of freedom which are restricted on complexation.²¹ Second, both guanidinium groups must bind only one phosphodiester linkage in a polyanionic RNA substrate. Finally, the cavity size should influence binding strength.²² Before examining the aminoimidazoline binding and catalysis, we will first present results from the analysis of receptors **1** and **2**.

Receptors **1** and **2** contain protonated 2-aminopyridine groups as mimics of guanidinium groups. These groups do not remain protonated at neutral pH in water; therefore, these receptors were studied in a low dielectric medium: chloroform.²³ Although significant aggregation of both the hosts and guests in this medium was observed and complicated the analyses, several conclusions about the effects of the size of the binding cavity and hydrogen bond strengths could be drawn. Receptor **2** binds dibenzyl phosphoric acid with a binding free energy approximately 1.4 kcal/mol larger than receptor **1**. The larger binding site in **2** allows for more linear hydrogen bonds between the host and guest, resulting in better complementarity and stronger binding. Given these results, we tested different binding site sizes in the bis-guanidinium receptors. However, the lesson did not directly apply.

The complementarity of the bis-guanidinium receptors for their phosphodiester guests yielded reasonably strong association constants in a variety of solvents. Since hydrolysis was the ultimate goal, water was the solvent of choice. However, binding constants of phosphodiesters with the bis-guanidinium receptors in pure water were determined to be very weak ($K_a < 5 \text{ M}^{-1}$), and therefore DMSO was added to the water to increase binding strength. Initially, we designed, synthesized, and evaluated a cleft composed of an octahydroacridine spacer with two aminoimidazoline groups preorganized to form a V-shaped cavity. The two aminoimidazoline groups were preorganized such that the guanidinium moieties converge toward each other and complex a phosphodiester via four hydrogen bonds. This binding strategy was meant to mimic the active site of the enzyme staphylococcal nuclease. In a 2:1 DMSO- d_6 :D₂O mixture, only 1-to-1 binding between **4** and dibenzyl phosphate was observed. The binding constant in this solvent system was $3.6 \times 10^2 \text{ M}^{-1}$. The binding constant increases to $8.0 \times 10^2 \text{ M}^{-1}$ in pure DMSO- d_6 ; however, 2-to-1 binding between **4** and dibenzyl phosphate was observed. The cooperativity of the two guanidinium groups of **4** was established by

comparing the association constant of dibenzyl phosphate and receptor **3**, which contains only one guanidinium group, with that of dibenzyl phosphate and **4**. Compound **3** had a binding constant of $3.3 \times 10^2 \text{ M}^{-1}$ for dibenzyl phosphate in pure DMSO. We also found that the tetraphenylborate salts of **4** and **6** bound dibenzyl phosphate more strongly than the chloride salts. These trends were expected, since it is well precedented that noncoordinating counterions and lower dielectric solvents will increase binding. However, our results were unexpected when using added salts in comparing the D,L and *meso* forms of **4** and **6**, and when comparing the influence of the cavity sizes in **4-5** and **6-7** on binding.

Since anions that can coordinate to a positively charged hydrogen bond donor often compete with an anionic guest for binding, we expected that the addition of salts such as LiCl, NaCl, and KCl would decrease binding. However, the exact opposite was observed. In a 2:1 DMSO- d_6 :D₂O solution, the addition of these salts to **4** resulted in larger binding constants to dibenzyl phosphate. LiCl had the most dramatic effect, while KCl had a smaller effect. Salts containing perchlorate and isocyanate decreased binding as expected. X-ray crystallographic analysis with **6** demonstrated that one chloride counterion was binding to one guanidinium group, creating a cavity with a water bridging to the phosphodiester bound with the other guanidinium group (Fig. 8A).²⁴ Although it is difficult to determine if this cooperativity between a chloride and a phosphodiester is occurring in solution, it would explain the increased binding constants with added chloride salts. To avoid the problem of a chloride bridging a guanidinium and a phosphodiester guest, we used a phosphomonoester guest so that charge neutrality would result during formation of the host-guest complex. Figure 8(B) shows the crystal structure of **6** and diphenyl phosphate. As anticipated, four linear and strong hydrogen bonds were present between the phosphoester and the host.

The size and shape of the binding cavity did not result in the trend of binding constants expected. We expected the *meso* isomers to have the best binding with dibenzyl phosphate because the guanidinium groups in **4** and **6** are on the same side of the spacer. The tetraphenylborate salts of the *meso* receptors gave the best binding constants, and of the chloride salts, the D,L isomer of **4** was best. We expected **6** to bind dibenzyl phosphate more effectively in high dielectric media due to its larger cavity size. Based on earlier studies, the binding constant increased as the cavity size increased from **1** to **2** in the binding of dibenzyl phosphoric acid in low dielectric media. The cavity in **6** is created using a hexahydrodicyclopenta[*b,e*]pyridine spacer, rather than an octahydroacridine spacer. Instead, **4** was the best receptor for dibenzyl phosphate. Flexibility in these systems arises from puckering of the cyclohexeno or cyclopenteno rings. The cyclopenteno rings allow envelope-type puckering modes, whereas the cyclohexeno rings allow each of the guanidinium groups to be

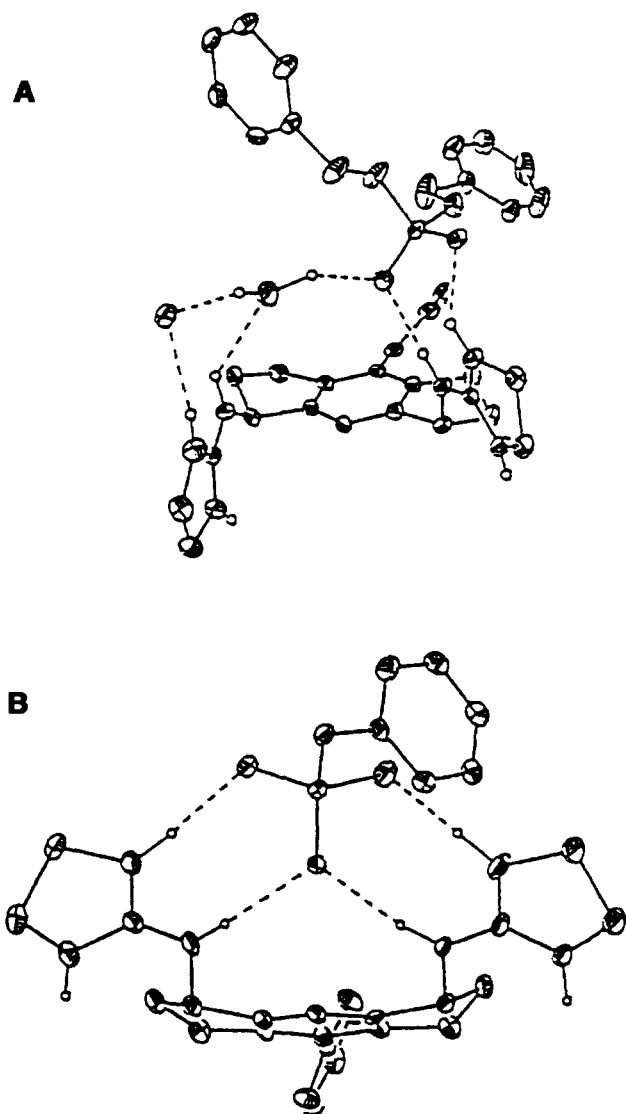


Figure 8. X-ray crystal structures of *meso*-**6**²⁵ (A) with chloride and dibenzyl phosphate counterions and (B) with phenyl phosphate.

either pseudo-axial or pseudo-equatorial. Our conclusion is that the flexibility of **4** allows this receptor to adopt a shape best suited for binding a phosphodiester, and that the rigidity imparted to **6** may not be optimal for complexation.

Catalysis

The cleavage/transesterification of RNA involves nucleophilic attack of the 2'-OH on an adjacent phosphodiester to create a dianionic trigonal bipyramidal phosphorane intermediate.²⁵ A common strategy to enhance the rate of this cleavage/transesterification is using electrophilic groups to coordinate to the phosphorane or general bases to assist nucleophilic attack.²⁶ In fact, almost all natural nucleases use both of these strategies. Staphylococcal nuclease has two guanidinium groups and a calcium which act as electrophilic activators. Hence, guanidinium groups alone may be expected to increase the rate of RNA cleavage/transesterification, albeit with much lower rate enhancements than when other catalytic moieties act in concert with them such as in an enzyme active site. Indeed, compound **4** is a catalyst for RNA hydrolysis.

Our initial studies involved the qualitative analysis of polyacrylamide gel electrophoresis of mRNA incubated with and without imidazole and with and without receptor **4**.²⁷ The imidazole was added as a general base to deliver the 2'-OH. Only the combination of imidazole and **4** resulted in cleavage/transesterification as displayed on the gel. The receptor was used in only 25 and 200 μM concentrations, thus demonstrating a high affinity for the RNA. If a control compound containing only one guanidinium group was used, no cleavage/transesterification was observed, indicating that cooperativity between two guanidinium groups is required for catalysis. We measured a 20-fold rate enhancement for receptor **4** with imidazole over imidazole alone using a kinetic assay that involves the quantitation of ³²P end-labeled RNA transcripts.

In order to determine whether guanidinium groups act either as electrostatic catalysts or as general acid catalysts in the formation of the phosphorane intermediate, the pK_a s of guanidinium groups and of phosphoranes must be compared. If the pK_a s of the conjugate acids of the phosphoranes are higher than the pK_a s of guanidiniums, then the guanidiniums are acting as general acids. Conversely, if the phosphorane pK_a s are lower than those of guanidiniums, then the guanidiniums are electrostatic catalysts. If the pK_a s are roughly matched, the possibility of low barrier hydrogen

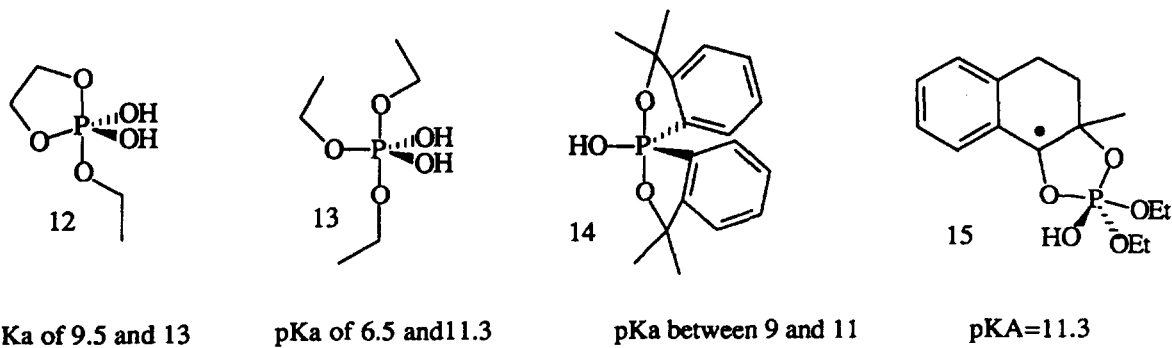


Figure 9. Estimated or measured pK_a values of phosphoranes.

bonds arise.²⁸ Unfortunately, the pK_a s of phosphoranes are in question.

Phosphorane pK_a s have been previously estimated, and in a few cases they have been experimentally determined (Fig. 9). Using the method of Branch and Calvin²⁹ (an empirical method), Westheimer estimated pK_a s of 9.5 and 13 for compound **12**.³⁰ Using heats of formation calculations, Guthrie estimated values of 6.5 and 11.3 for compound **13**.³¹ McClelland and Martin have experimentally determined the pK_a of a phosphorane derived from a phosphinic acid **14**; McClelland's value is between 9 and 10,³² while Martin's is between 10 and 11.³³ Using pulse radiolysis, we measured a pK_a of 11.3 for phosphorane **15** formed from a triester.³⁴ This pK_a should be similar to the first pK_a of a phosphorane derived from a diester. Since the pK_a s of diprotic and triprotic acids such as sulfuric and phosphoric acid are separated by four to five pK_a units, we would predict a second pK_a to be 15–16. Therefore we believe that the pK_a s of phosphoranes relevant to RNA cleavage/transesterification are about 11 and 15. However, given the fact that the heats of formation method used by Guthrie has proven accurate with hemiotho ester pK_a s,³⁵ as well as the large variation of pK_a values in the literature, we do not consider this issue settled. Thus our group is actively designing and implementing experiments to measure phosphorane pK_a s. Even though we feel that the issue of phosphorane pK_a s is not totally settled, we can use the current literature values to predict the ability of nuclease active site residues, including guanidinium groups, to act as either electrostatic or as general-acid catalysts.

Our pK_a values, as well as those of Guthrie and Westheimer, predict that the imidazolium of histidine should be a general acid when in proximity to and if properly positioned near a dianionic phosphorane. Such a postulate is being currently debated for RNase A.³⁶ In support of this prediction, a proton inventory study on an enzyme model consisting of β -cyclodextrin with two appended imidazoles has clearly indicated proton transfer from an imidazolium to a developing phosphorane intermediate.³⁷

An ammonium group should act as a general acid, given any of the estimated, and now measured, phosphorane pK_a values. Lysine has recently been proposed as a potential low-barrier hydrogen bond donor during the catalysis of RNA cleavage by RNase A.²⁷ Such a hydrogen bond is postulated to form when the pK_a of the enzyme hydrogen bond donor is matched to the pK_a of the conjugate acid of the transition state hydrogen bond acceptor. These hydrogen bonds are thought to be worth as much as 31 kcal/mol in the gas phase.³⁸ As yet there is no definitive proof of these hydrogen bonds at enzyme active sites.³⁹ Although enzyme active sites are known to shift pK_a values from those in solution,⁴⁰ and our measured pK_a values are for the phosphorane intermediate not the transition state (which would be expected to have lower pK_a s), it would seem that pK_a values near 11 and 15 are too high to allow for the

formation of a low-barrier hydrogen bond with the lysine side chain (pK_a 10.4).

Most intriguing is the potential new role for guanidinium groups at enzyme active sites. The guanidinium group has been postulated to play at least three roles in nuclease-mediated hydrolysis.¹ First, the ditopic nature of the hydrogen-bonding pattern can bind and orient a phosphoester substrate. Second, the positive charge allows for electrostatic stabilization of anionic phosphorane-like transition states. Third, proton transfer to phosphorane leaving groups (whose pK_a s are near 14.8)⁴¹ may occur.⁴² Given our phosphorane pK_a s, guanidinium groups (with pK_a s near 13) should also act as general acids and therefore protonate phosphoranes. In this scenario, an arginine could act as both a general acid and base to shuttle protons on and off the phosphorane intermediates formed along the hydrolysis pathway.

For example, in SNase the guanidiniums have been shown to contribute approximately $10^{4.6}$ to a total 10^{16} -fold rate enhancement over background.^{42b} It is noteworthy that the guanidinium pK_a is bracketed by the phosphorane pK_a s. Therefore in SNase, a phosphorane that results from the hydrolysis of RNA or DNA may deprotonate a coordinated guanidinium, yielding a monoanionic-monoprotic phosphorane (Fig. 10). This protonation state could be used to lower the barrier to nucleophilic attack, while subsequent deprotonation could be used to lower the barrier to leaving group departure. Such a 'push-pull' mechanism would best be facilitated by a functional group with a pK_a close to that of the intermediate phosphorane, such as a guanidinium.

Our measured phosphorane pK_a values also shed light on the potential for low-barrier hydrogen bonds with guanidiniums. As mentioned earlier, functional group pK_a s are often significantly perturbed at enzyme active sites from their values in solution.⁴⁰ One would therefore predict that the pK_a s of intermediates could be

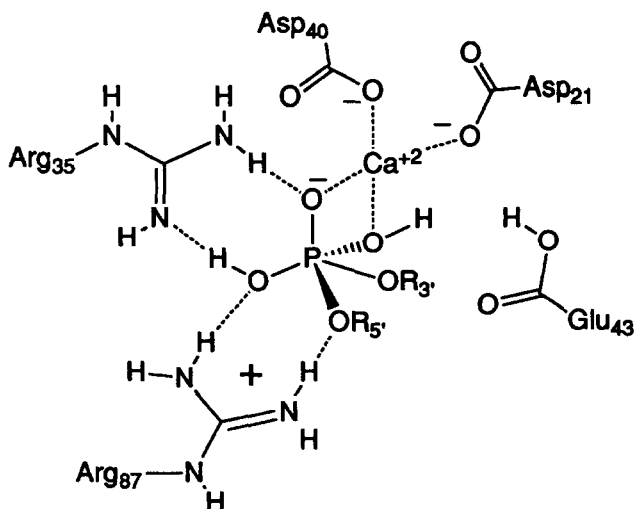


Figure 10. View of a phosphorane bound within the active site of SNase demonstrating proton transfer from a guanidinium.

significantly shifted in local microenvironments. For example, coordination of phosphoranes to other nuclease electrophiles would depress the phosphorane pK_a s. However, the similarity between phosphorane and guanidinium pK_a s leads one to postulate that guanidiniums are best suited as low barrier hydrogen bond partners for phosphoranes. If low-barrier hydrogen bonds prove to be valid species, such pK_a matching could be responsible for the majority of the $10^{4.6}$ -fold rate enhancement imparted by the SNase arginines.

Jencks' 'libido rule'⁴³ states that the driving force for general-acid catalysis results from switching a thermodynamically unfavorable proton transfer in the ground state to a thermodynamically favorable one in the transition state. It would follow that the larger the pK_a difference between the ground and transition states, the larger the potential driving force for general-acid catalysis. A large pK_a difference exists between the ground state (near 1) and the phosphorane intermediate (near 11 and 15). However, the general acid needs to have a pK_a between these two extremes, unlike the low-barrier hydrogen bond theory involving matched transition state and general acid pK_a s.⁴⁴ Given the phosphorane pK_a values of 11 and 15, one would expect nuclease histidines or lysines to be much more likely to act as general acids than arginines, whereas arginines would be more effective at forming low-barrier hydrogen bonds. The key difference between the libido rule and the low-barrier hydrogen bond theory is the distance between the heteroatoms involved in the hydrogen bonding and proton transfer. A low-barrier hydrogen bond is formed at distances of 2.4 Å or less. Low-barrier hydrogen bonds are likely formed when the distances between the hydrogen bonding partners are this short, whereas simple general-acid catalysis should favor longer distances. Future experiments involving phosphorane-like transition states and general acids will help to delineate the difference between general acid catalysis and low-barrier hydrogen bonds as a function of the distance of the two hydrogen bonding groups.

Catalyst improvements

Our catalysts 4–8 were initially designed to complement the tetrahedral nature of a phosphodiester to ensure strong binding in highly competitive solvents. Strong binding of the guest ground state is not necessarily the best strategy for catalysis; rather, the binding of the transition state should be our main focus. Currently, we are developing receptors with a certain amount of flexibility which will allow for re-organization of the catalytic moieties during the cleavage/transesterification reaction. The advantages of this strategy include not only maximizing the host–guest ground state binding but also stabilizing the transition states and intermediates along the reaction pathway.

Through information gained by research and advances in the field of phosphodiester hydrolysis, we have set out to increase the rate enhancements of our receptors

through the incorporation of additional catalytic groups. Our goal is to synthesize a series of new receptors possessing intramolecular general bases or metals that are preorganized with guanidinium groups to cooperatively bind phosphodiester and enhance their hydrolysis rates. A spacer that will hold several functional groups on the same face of a platform thus creating a cavity for which to bind the phosphoester was required. Since we wished to evaluate the effect of each functional group, the effect of various combinations of functional groups, and various positions of the functional groups, a very versatile spacer that could be easily derivatized was required. After considering several designs, we chose compound 9 as our spacer.

Compound 10 is a triaminomethyl triethylbenzene derivative whose preorganization is derived from alternating steric bulk around the benzene in order to present the three catalytic moieties on the same face of the spacer. Previous studies of similar systems found a 12 kcal/mol preference for the all-alternating structure.⁴⁵ Selective derivatization of the amine groups of 9 allows for the convergence of one, two, or three different functional groups to form a binding pocket. In the design of a bis-guanidinium catalyst incorporating a general base, only two of the amines were converted to guanidinium groups while the third amine was left alone. Figure 11 shows the proposed mechanism of catalysis of RNA cleavage/transesterification with 10. Compound 8 was also developed for studying the cooperativity of a general base and two guanidinium groups.

The synthesis of 8 is shown in Figure 12. The synthesis is based on the syntheses of 6 and 7²⁴ and began with the condensation of *o*-anisaldehyde, cyclopentanone, and ammonium acetate to give the dibenzylidene 16. The dibenzylidene 16 in dichloromethane was then treated with ozone to yield the diketone 17 in good yield. The dione 17 was then converted to the dioxime 18 using hydroxylamine hydrochloride and potassium carbonate

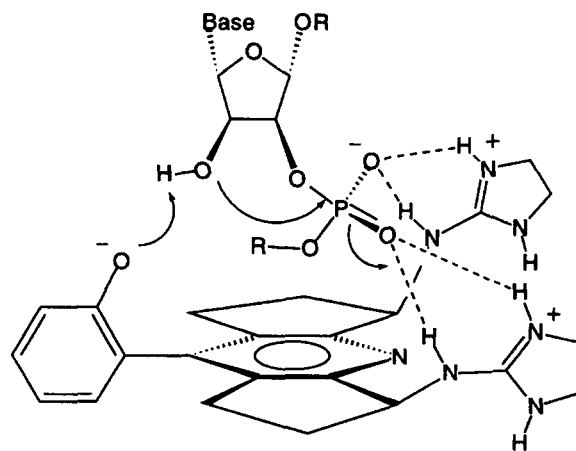


Figure 11. Mechanistic view of the hydrolysis of an RNA phosphodiester by 8. Molecular modeling demonstrates that the phenoxide and 2'-OH are within hydrogen-bonding distance. However, for clarity of presentation they are not drawn to scale.

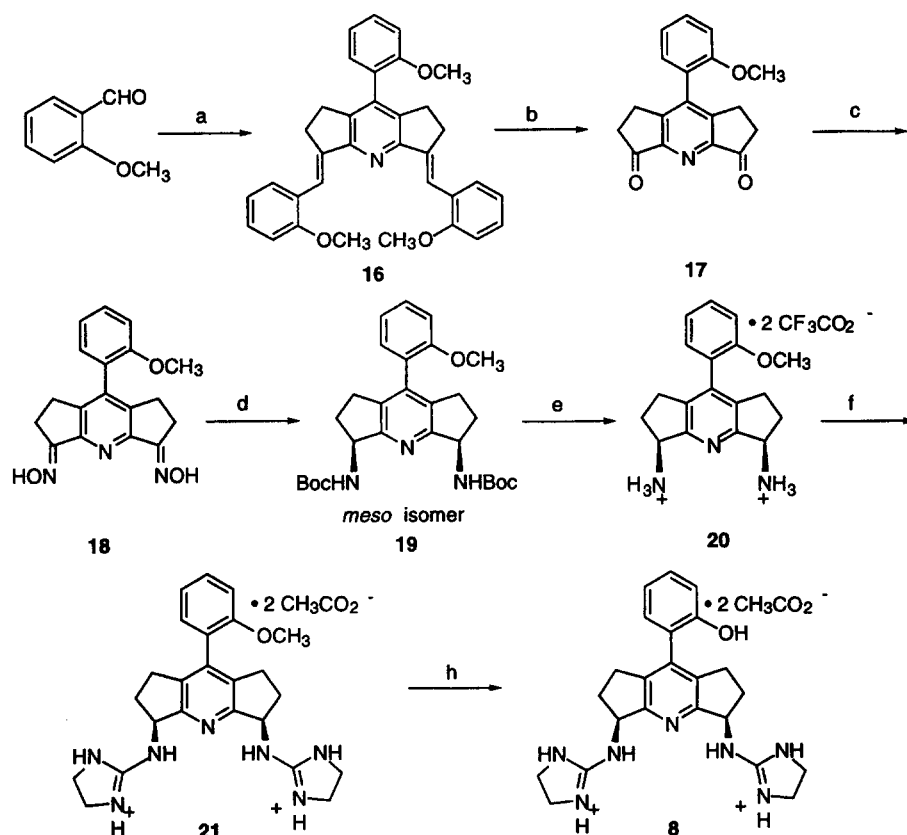


Figure 12. Synthesis of **8**. Reagents and conditions: (a) Cyclopentanone, NH_4OAc , EtOH, reflux, 10–30 min (15%); (b) (i) $\text{O}_3, \text{CH}_2\text{Cl}_2$, -78°C ; (ii) $(\text{CH}_3)_2\text{S}$ (76%); (c) $\text{NH}_2\text{OH}\cdot\text{HCl}$, Na_2CO_3 , DMF, 85°C , 4 h (87%); (d) (i) NaBH_4 , TiCl_4 , 0°C –rt, 72 h; (ii) Boc_2O , CHCl_3 , rt, 6 h; (iii) separation of diastereomers (8% *meso* isomer from **18**); (e) TFA, H_2O , 4 h (83%); (f) 2-methylthio-2-imidazole, solid melt, 100°C , 4 days (19%); (g) 48% aq HBr, HOAc, reflux, 13 h (95% purity).

in DMF. The reduction to the diastereomeric mixture of amines was effected with sodium borohydride and titanium tetrachloride in dimethoxyethane. Protection of the amines with di-*t*-butyl dicarbonate in chloroform facilitated the purification as well as isolation of the diastereomers of **19**. From this point on, we continued the synthesis solely with the *meso* isomer. Deprotection of the amines with trifluoroacetic acid in water yielded the trifluoroacetate salt **20**, which was combined with 2-methylthio-2-imidazole and subjected to solid melt conditions to give the bis-guanidinium compound **21**.⁴⁶ The final step was the unmasking of the intramolecular general base phenol. This was accomplished using 48% hydrobromic acid in refluxing glacial acetic acid in high yield.⁴⁷ This catalyst **8** may use a phenoxide to deliver the RNA 2'-OH. In order to effect catalysis at physiological pH (near 7), one should use a general base whose conjugate acid has a pK_a near 7. Both the amine and phenoxide in **10** and in **8**, respectively, have pK_a s of their conjugate acids near 9. We will have to lower these pK_a s by about two units to have catalysis at physiological pH, but compounds **8** and **10** will allow us to analyze the cooperativity between guanidiniums and general bases, albeit not at the optimal pH for practical applications. These studies are currently in progress and will be reported in due course.

We are also examining the cooperativity of metals with guanidiniums for the catalytic cleavage/transesterifica-

tion of RNA. Figure 13 shows our first design. Zinc is the metal of choice since it is very commonly found in nucleases, and it is known to act in concert with guanidinium groups in the enzyme alkaline phosphatase.⁴⁸ The design of **11** incorporates a tridentate metal-binding ligand, which is preorganized in such a manner that the metal points into the cavity and should converge with the two guanidinium groups on a bound phosphodiester. Studies using this compound as a catalyst of RNA cleavage/transesterification are currently underway and will be reported in due course.

Summary

The guanidinium functional group is commonly used in nature to recognize and bind anions through ion pairing and hydrogen bonding. Analysis of simple salts reveals a variety of features found in natural systems, including phosphodiesterases and RNA recognition motifs. Further, the guanidinium group has been postulated to play at least three roles in RNA hydrolysis. First, the ditopic nature of the hydrogen-bonding pattern can bind and orient a phosphoester substrate. Second, the positive charge allows for electrostatic stabilization of anionic phosphorane-like transition states. Third, proton transfer to phosphorane leaving groups may occur. In order to determine whether guanidinium groups act either as electrostatic catalysts or as general-acid

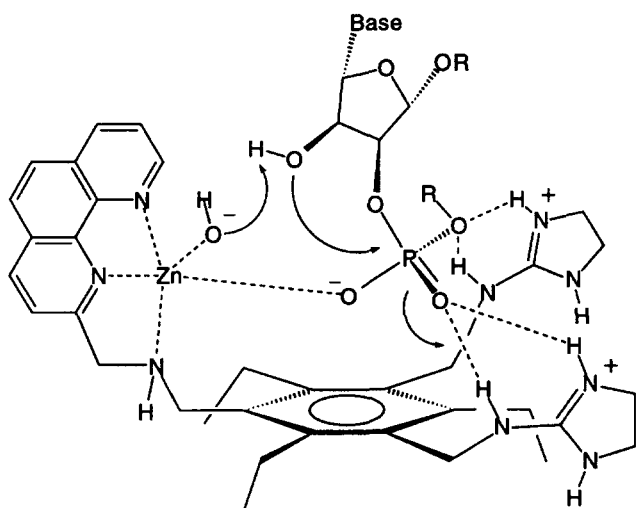


Figure 13. Schematic representation of the hydrolysis of RNA using **12**. Once again, for clarity of presentation, the hydrogen-bond distances are not drawn to scale.

catalysts in the formation of the phosphorane intermediate, the pK_a s of guanidinium groups and of phosphoranes must be compared. Our group is actively designing and implementing experiments to measure phosphoranes pK_a s. From our current pK_a measurements, guanidinium groups should act as general acids and therefore protonate phosphoranes.

We have constructed 11 molecules to explore some of these features. We have used four-point hydrogen bonding to orient a phosphodiester within a binding cavity and to activate electrophilically the phosphodiester toward cleavage/transesterification. We measured a 20-fold rate enhancement for receptor **4** with imidazole over imidazole alone using a kinetic assay that involves the quantitation of ^{32}P end-labeled RNA transcripts. The phosphorane transition state is stabilized by ion pairing/guanidinium general-acid proton transfer from **4**. These results demonstrate that guanidinium groups in a totally synthetic system can act as electrophilic activators of phosphodiesters. Expanding on receptors **4–7**, receptors **8** and **10** both have an intramolecular general base and receptor **11** has a metal binding site to complement the bis-guanidinium functionality. In conclusion, we are focusing our efforts on increasing the rate enhancement and deciphering the details of the mechanism of hydrolysis, as well as the energetic stabilization that the bis-guanidinium receptors impart to phosphodiester hydrolysis.

Experimental

Synthesis—general considerations

^1H and ^{13}C NMR spectra were obtained in CDCl_3 , CD_3CN , $\text{DMSO}-d_6$, CD_3OD , or D_2O used as purchased. Spectra were recorded on a General Electric QE-300 (300 MHz), a Bruker AC-250 (250 MHz), a Bruker

AMX-500 (500 MHz), or a Varian Unity Inova (500 MHz) spectrometer. Melting points were measured on Thomas Hoover capillary melting-point apparatus and are uncorrected. Low-resolution and high-resolution mass spectra were measured with Finnigan TSQ70 and VG Analytical ZAB2-E instruments, respectively.

Preparative flash chromatography was performed on Scientific Adsorbents Incorporated Silica Gel 40 mm. Analytical thin-layer chromatography was performed on precoated Silica Gel 60 F-254 plates. Cation exchange and reversed-phase liquid chromatography (LC) were performed on Sephadex-CM C-25 ion-exchange resin 40–120 mm and RP 18 C18-modified silica gel 55–105 mm, respectively, using a Pharmacia LKB-FRAC-100 LC system. Solvents and reagents were purchased from Aldrich, Spectrum, Sigma, and Mallinckrodt and used without purification, unless otherwise stated. Dimethoxyethane was distilled from sodium benzophenone ketyl. Ozone was generated by a Welsbach T-816 ozone generator at 90 V at 1.5 L/min.

3,5-Dibenzylidene-1,2,3,5,6,7-hexahydro-8-(2-methoxyphenyl)dicyclo-penta[b,e]pyridine (16). Ammonium acetate (19.4 g, 250 mmol) was dissolved in absolute EtOH (250 mL). Cyclopentanone (23.0 mL, 260 mmol) and *o*-anisaldehyde (68.0 g, 500 mmol) were combined and added together to the mixture, which turned yellow immediately on addition and to dark red with gentle heating. On reflux or shortly thereafter, a precipitate formed. Heating was continued for another 10 min at which point the mixture was removed from the heat and cooled to just above rt, then on ice for 30 min. The loose precipitate was collected via suction filtration. The hard polymer-like material was broken into small pieces, and all of the solid was dissolved in CH_2Cl_2 (250 mL). Hexanes were then added to precipitate the product. This solid was also collected and air-dried overnight. Another two crops were collected from later crystal growth to give 20 g (15%) of methyl ether **16** as a yellow powder: mp 218–220 °C (dec); ^1H NMR (250 MHz, CDCl_3) δ 7.9 (s, 2H, C=CHAr), 7.6–6.7 (comp, 12H, Ar), 3.9 (s, 6H, OCH_3); 3.7 (s, 3H, OCH_3), 3.1 (m, 4H, CH_2CH_2), 2.7 (m, 4H, CH_2CH_2); ^{13}C NMR (62.8 MHz, CDCl_3) δ 160.4, 157.5, 156.1, 142.3, 140.6, 137.8, 129.6, 129.3, 128.7, 127.8, 127.3, 125.9, 120.5, 120.0, 116.3, 111.0, 110.4, 55.4, 55.3, 29.2, 27.3; CIHRMS m/z 502.237 ($\text{M}^+ + \text{H}$, $\text{C}_{34}\text{H}_{32}\text{NO}_3$ requires 502.238).

3,5-Dioxo-1,2,3,5,6,7-hexahydro-8-(2-methoxyphenyl)-dicyclopenta[b,e]pyridine (17). Dibenzylidene **16** (5.00 g, 9.97 mmol) was dissolved in CH_2Cl_2 (300 mL). The yellow mixture was cooled to -78 °C and then was treated with ozone (excess) until a green color persisted for 2 min (16 min). Oxygen was passed through the system to purge excess ozone (3 min). Dimethyl sulfide (2.6 mL, 35.0 mmol) was added via syringe. The reaction mixture was allowed to warm to rt with stirring overnight. The solvent was removed by rotary evaporation to yield a dark brown residue. The residue was purified by flash column chromatography with gradient elution of 90:10 EtOAc:hexanes (v/v) to 100% EtOAc.

The compound at $R_f = 0.48$ was isolated to give 2.21 g (76%) of diketone **17** as a tan solid on removal of solvent: mp 202–203 °C; $^1\text{H NMR}$ (250 MHz, CDCl_3) (7.53–7.08 (comp, 4H, Ar), 3.80 (s, 3H, OCH_3), 3.04–2.98 (m, 4H, CH_2CH_2), 2.82–2.77 (m, 4H, CH_2CH_2); $^{13}\text{C NMR}$ (62.8 MHz, CDCl_3) δ 204.2, 155.9, 155.3, 151.9, 145.8, 131.0, 129.3, 121.9, 121.0, 111.4, 55.4, 50.6, 35.5, 22.8; CIHRMS m/z 294.1135 ($\text{M}^+ + \text{H}$, $\text{C}_{18}\text{H}_{16}\text{NO}_3$ requires 294.1130).

3,5-Bis(hydroxyimino)-1,2,3,5,6,7-hexahydro-8-(2-methoxyphenyl)-dicyclopenta[*b,e*]pyridine (18). Diketone **17** (2.21 g, 7.56 mmol), $\text{NH}_2\text{OH}\cdot\text{HCl}$ (4.85 g, 69.8 mmol), and Na_2CO_3 (4.48 g, 42.2 mmol) were taken up in DMF (35 mL). The mixture was stirred with gentle heating (bath temperature 85 °C) for 4 h. Heating was stopped, and the solvent was removed under high vacuum overnight. The tan residue was taken up in H_2O (100 mL) and stirred at 0 °C for 2 h. The solid that precipitated was collected via suction filtration, then washed with cold Et_2O and allowed to air dry to yield 2.14 g (87%) of dioxime **18** as a tan solid: mp 230 °C (dec); $^1\text{H NMR}$ (250 MHz, $\text{DMSO-}d_6$) δ 11.1 (bs, 2H, C=NOH), 7.47–7.02 (m, 4H, Ar), 3.74 (s, 3H, OCH_3), 2.75–2.66 (comp, 8H, CH_2CH_2); $^{13}\text{C NMR}$ (62.8 MHz, $\text{DMSO-}d_6$) δ 159.5, 155.6, 155.2, 141.7, 130.2, 129.4, 123.5, 120.5, 111.6, 55.4, 24.7, 24.5; CIHRMS m/z 324.1349 ($\text{M}^+ + \text{H}$, $\text{C}_{18}\text{H}_{18}\text{N}_3\text{O}_3$ requires 324.1348).

Meso-3,5-bis[(1,1-dimethylethoxy)carbonyl]amino]-1,2,3,5,6,7-hexahydro-8-(2-benzyloxyphenyl)dicyclopenta[*b,e*]pyridine (19). NaBH_4 (2.42 g, 63.9 mmol) and TiCl_4 (3.6 mL, 32.8 mmol) were added to a flame-dried 250-mL round bottomed flask in a dry box. Dry DME (50 mL) was added to the mixture at 0 °C. A wide-bore needle was used to vent HCl (g). The mixture was stirred at 0 °C for 15 min, at which point dioxime **18** (2.14 g, 6.62 mmol) was added. The mixture became brown and was allowed to warm to rt with stirring for 72 h. The mixture was cooled to 0 °C and quenched with aq sodium tartrate (2.70 g tartaric acid in 100 mL 1 M NaOH). On addition, the mixture turned dark blue. The mixture was extracted with CH_2Cl_2 (1000 mL) and brine to break up the emulsion and dried (Na_2SO_4). The combined organic extracts were concentrated to give 1.63 g (83% crude yield) as a tan residue, which was dried under high vacuum overnight. The crude diamine (1.63 g, 5.52 mmol) and di-*tert*-butyl dicarbonate (2.84 g, 13.0 mmol) were dissolved in CHCl_3 (80 mL). The reaction mixture was stirred for 6 h at rt under Ar. The solvent was removed under reduced pressure. The compound was purified by flash column chromatography with gradient elution of 40:60 to 50:50 (v/v) EtOAc :hexanes. The compound at $R_f = 0.71$ was isolated to give 0.27 g (8.3% from **18**) of *meso*-dicarbamate **19** as a white solid: mp 110–116 °C; $^1\text{H NMR}$ (250 MHz, CDCl_3) δ 7.35 (t, 1H, Ar), 7.09–6.95 (comp, 3H, Ar), 5.27 (bs, 2H, $\text{NHCOC}(\text{CH}_3)_3$), 4.96 (bs, 2H, $\text{PyrCHNHCOC}(\text{CH}_3)_3$), 3.75 (s, 3H, OCH_3), 2.74–2.58 (comp, 6H, CH_2CH_2), 1.89–1.84 (comp, 2H, CH_2CH_2), 1.46 (s, 18H, $\text{NHCOC}(\text{CH}_3)_3$); $^{13}\text{C NMR}$ (62.8 MHz, CDCl_3) δ 161.1, 156.2, 155.8, 155.4, 140.9,

135.3, 135.1, 129.7, 129.7, 129.4, 124.9, 124.8, 120.4, 120.3, 110.8, 79.2, 56.2, 55.1, 33.5, 33.5, 28.3, 26.7, 26.5, 26.2; CIHRMS m/z 496.2816 ($\text{M}^+ + \text{H}$, $\text{C}_{28}\text{H}_{38}\text{N}_3\text{O}_5$ requires 496.2811).

Meso-3,5-diamino-1,2,3,5,6,7-hexahydro-8-(2-methoxyphenyl)-dicyclopenta[*b,e*]pyridine dihydrodinitriferuoroacetate (20). The *meso*-dicarbamate **19** (459 mg, 0.92 mmol) was dissolved in TFA (2 mL) and H_2O (2 mL) and was stirred at rt for 4 h. The volatiles were removed under vacuum. H_2O was added to the residue and the solution was lyophilized until a constant weight was achieved to give 405 mg (83%) of dihydrodinitriferuoroacetate salt **20** as a fluffy pink solid: mp 185 °C (dec.); $^1\text{H NMR}$ (250 MHz, CDCl_3) δ 7.44 (t, 1H, Ar), 7.19–7.02 (comp, 3H, Ar), 4.78 (t, 2H, PyrCHNH_3^+), 3.76 (s, 3H, OCH_3), 2.90–2.62 (comp, 6H, CH_2CH_2), 2.16–2.02 (comp, 2H, CH_2CH_2); $^{13}\text{C NMR}$ (62.8 MHz, CDCl_3) δ 163.2 (q, $J_{\text{CF}} = 34.7$ Hz), 159.4, 159.3, 157.6, 157.1, 143.7, 143.7, 138.2, 138.2, 131.6, 130.3, 130.4, 125.2, 121.7, 120.4 (q, $J_{\text{CF}} = 291$ Hz), 112.4, 112.4, 56.2, 55.8, 30.0, 29.9, 27.9, 27.8; CIHRMS m/z 296.174 ($\text{M}^+ + \text{H}$, $\text{C}_{18}\text{H}_{22}\text{N}_3\text{O}$ requires 296.176).

Meso-*N,N'*-bis(4,5-dihydro-1H-imidazol-2-yl)-1,2,3,5,6,7-hexahydro-8-(2-methoxyphenyl)dicyclopenta[*b,e*]pyridine-3,5-diamine dihydrodiacetate (21). Dihydrodinitriferuoroacetate salt **20** (405 mg, 0.773 mmol) and 2-methylthio-2-imidazoline (191 mg, 1.64 mmol) were ground separately and then together with a mortar and pestle and pressed into a 1-mL conical vial. The vial was sealed and heated in an oil bath at 100 °C for four days. The mixture was cooled to rt. Dilute acetic acid (5% v/v) was added to the mixture. Additional acid and H_2O (10 mL) were added and the mixture was lyophilized. Purification by RPLC with gradient elution from 100% 25 mM NH_4OAc to 100% CH_3CN , followed by cation exchange on Sephadex with gradient elution from 25 mM to 1 M NH_4OAc gave 82 mg (19%) of dihydrodiacetate salt **21** as a light-red solid: 61 °C (morphology change), 86 °C (dec); $^1\text{H NMR}$ (500 MHz, CD_3OD) δ 7.45 (comp, 1H, Ar), 7.18–7.03 (comp, 3H, Ar), 4.99 (m, 2H, $\text{PyrCH}_2\text{Guan}$), 3.76 (s, 11H, OCH_3 and $\text{HNCH}_2\text{CH}_2\text{NH}$), 2.88–2.58 (comp, 6H, CH_2CH_2), 2.06–1.96 (comp, 2H, CH_2CH_2), 1.87 (s, 6H, CH_3COO^-); $^{13}\text{C NMR}$ (125 MHz, CD_3OD) δ 179.4, 179.4, 161.9, 161.9, 161.8, 161.5, 161.5, 161.3, 157.6, 157.5, 157.3, 153.4, 137.7, 137.6, 137.5, 137.2, 131.6, 130.6, 130.3, 130.4, 125.5, 121.8, 112.5, 59.2, 59.1, 59.1, 55.9, 55.8, 44.1, 32.7, 32.6, 32.5, 32.5, 27.8, 27.7, 27.6; CIHRMS m/z 432.250 ($\text{M}^+ + \text{H}$, $\text{C}_{24}\text{H}_{30}\text{N}_7\text{O}$ requires 432.251).

Meso-*N,N'*-bis(4,5-dihydro-1H-imidazol-2-yl)-1,2,3,5,6,7-hexahydro-8-(2-hydroxyphenyl)dicyclopenta[*b,e*]pyridine-3,5-diamine dihydrodiacetate (8). The dihydroacetate salt **21** (9.6 mg, 0.014 mmol) was dissolved in 48% aqueous hydrobromic acid (1 mL) and glacial acetic acid (1 mL) and stirred at reflux for 13 h. The mixture was cooled to rt and the volatiles were removed under high vacuum. The product was isolated by cation exchange on Sephadex with gradient elution of 25 mM to 1 M NH_4OAc to give 6.4 mg (95% purity) of

dihydrodiacetate salt **8** as a white solid: mp 185 °C (dec); ¹H NMR (500 MHz, CD₃CN) δ 7.25 (comp, 1H, Ar), 7.10–6.88 (comp, 3H, Ar), 4.89 (t, 2H, PyrCH₂Guan), 3.71 (s, 8H, HNCH₂CH₂NH), 2.84–2.53 (comp, 6H, CH₂CH₂), 2.09–1.96 (comp, 2H, CH₂CH₂), 1.79 (bs, 6H, CH₃COO⁻); ¹³C NMR (125 MHz, CD₃CN) δ 180.0, 175.4, 170.1, 162.3, 162.2, 161.7, 161.4, 161.3, 155.5, 155.4, 155.3, 144.1, 143.8, 137.9, 137.7, 137.4, 137.2, 131.5, 131.5, 131.3, 131.0, 130.9, 124.2, 120.9, 117.5, 117.4, 117.2, 59.2, 59.1, 44.7, 44.2, 42.1, 32.6, 32.5, 28.1, 28.0, 27.9, 24.7, 24.0, 19.0, 16.8; CIHRMS *m/z* 418.2350 (M⁺+H, C₂₃H₂₈N₇O requires 418.2355).

Acknowledgements

We gratefully acknowledge financial support for this project from the National Institutes of Health and the Robert A. Welch Foundation. In addition, we wish to thank Dr Axel Metzger for assistance with synthetic strategy.

References

- For a more comprehensive review on guanidinium receptors and artificial receptors see: Hannon, C. L.; Anslyn, E. V. *Bioorganic Chemistry Frontiers*; Dugas, H., Ed.; Springer: Berlin, 1993; Vol. 3, Ch. 6.
- (a) Sawka-Dobrowolsky, W.; Glowiak, T.; Tyka, R. *Acta Crystallogr.* **1984**, C40, 174. (b) Aoki, K.; Nagano, K.; Iitaka, Y. *Acta Crystallogr.* **1971**, B27, 11. (c) Salunke, D. M.; Vijayan, M. *Acta Crystallogr.* **1982**, B38, 1328. (d) Sudhakar, V.; Vijayan, M. *Acta Crystallogr.* **1980**, B36, 120. (e) Berthou, P. J.; Laurent, A.; Nakajima, S. *Acta Crystallogr.* **1976**, B32, 1529. (f) Maeda, T.; Fujiwara, T.; Tomita, K.-i. *Bull. Chem. Soc. Jpn.* **1972**, 45, 3628. (g) Steward, E. G.; Warner, D.; Clarke, G. R. *Acta Crystallogr.* **1974**, B30, 813.
- Karle, I. L.; Karle, J. *Acta Crystallogr.* **1964**, A17, 835.
- Cotton, F. A.; Day, V. W.; Hazen, E. E. Jr.; Larsen, S.; Wong, S. T. K. *J. Am. Chem. Soc.* **1974**, 96, 4471.
- Calnan, B. J.; Tidor, B.; Biancalana, S.; Hudson, D.; Frankel, A. D. *Science (Washington, DC)* **1991**, 252, 1167.
- Curtis, R. M.; Pasternak, R. A. *Acta Crystallogr.* **1955**, A8, 675.
- Adams, J. M.; Small, R. W. H. *Acta Crystallogr.* **1976**, B32, 832.
- (a) Dingwall, C.; Ernberg, I.; Gait, M. J.; Green, S. M.; Heaphy, S.; Karn, J.; Lowe, A. D.; Singh, M.; Skinner, M. A. *EMBO J.* **1990**, 9, 4145. (b) Roy, S.; Dellling, U.; Chen, C.-H.; Rosen, C. A.; Sonenberg, N. *Genes Dev.* **1990**, 4, 1365. (c) Cordingley, M. G.; LaFemina, R. L.; Callahan, P. L.; Condra, J. H.; Sardana, V. V.; Graham, D. J.; Nguyen, T. M.; LeGrow, K.; Gotlib, L.; Schlabach, A. J.; Colonna, R. J. *Proc. Natl. Acad. Sci. U.S.A.* **1990**, 87, 8985.
- Frankel, A. D. *Curr. Opin. Genet. Dev.* **1992**, 2, 293.
- Tao, J.; Frankel, A. D. *Proc. Natl. Acad. Sci. U.S.A.* **1992**, 89, 2723.
- Puglisi, J. D.; Tan, R.; Calnan, B. J.; Frankel, A. D.; Williamson, J. R. *Science (Washington, DC)* **1992**, 257, 76.
- Puglisi, J. D.; Chen, L.; Frankel, A. D.; Williamson, J. R. *Proc. Natl. Acad. Sci. U.S.A.* **1993**, 90, 3680.
- (a) Levitt, M. *Nature (London)* **1969**, 224, 759. (b) Giegé, R.; Puglisi, J. D.; Florentz, C. In *Prog. Nucleic Acid Res. Mol. Biol.*; Cohn, W. E.; Moldave, K., Eds.; Academic: New York, 1993; Vol. 45, pp 129–206.
- (a) Michel, F.; Westhof, E. *J. Mol. Biol.* **1990**, 216, 585. (b) Chastain, M.; Tinoco, I., Jr. *Biochemistry* **1992**, 31, 12733.
- Yarus, M.; Majerfeld, I. *J. Mol. Biol.* **1992**, 225, 945.
- Yarus, M. *Science (Washington, DC)* **1988**, 240, 1751.
- Wyatt, J. R.; Chastain, M.; Puglisi, J. D. *BioTechniques* **1991**, 11, 764.
- Cotton, F. A.; Hazen, E. E., Jr.; Legg, M. J. *Proc. Natl. Acad. Sci. U.S.A.* **1979**, 76, 2551.
- Serpensu, E. H.; Shortle, D.; Mildvan, A. S. *Biochemistry* **1987**, 26, 1289.
- Weber, D. J.; Gittis, A. G.; Mullen, G. P.; Abeygunawardana, C.; Lattman, E. E.; Mildvan, A. S. *Proteins* **1992**, 13, 275.
- Cram, D. J. *Angew Chem. Int. Ed. Engl.* **1986**, 25, 1039.
- Perreault, D. M.; Chen, X.; Anslyn, E. V. *Tetrahedron* **1995**, 51, 353.
- Chu, F.; Flatt, L. S.; Anslyn, E. V. *J. Am. Chem. Soc.* **1994**, 116, 4194.
- Kneeland, D. M.; Ariga, K.; Lynch, V. M.; Huang, C.-Y.; Anslyn, E. V. *J. Am. Chem. Soc.* **1993**, 115, 10042.
- Breslow, R.; Labelle, M. *J. Am. Chem. Soc.* **1986**, 108, 2655.
- For some representative examples see: (a) Chin, J. *Acc. Chem. Res.* **1991**, 24, 145. (b) Koike, T.; Kimura, E. *J. Am. Chem. Soc.* **1991**, 113, 8935. (c) Jubian, V.; Dixon, R. P.; Hamilton, A. D. *J. Am. Chem. Soc.* **1992**, 114, 1120. (d) Morrow, J. R.; Buttrey, L. A.; Shelton, V. M.; Berback, K. A. *J. Am. Chem. Soc.* **1992**, 114, 1903. (e) Bashkin, J. K.; Frolova, E. I.; Sampath, U. *J. Am. Chem. Soc.* **1994**, 116, 5981. (f) Magda, D.; Miller, R. A.; Sessler, J. L.; Iverson, B. L. *J. Am. Chem. Soc.* **1994**, 116, 7439. (g) Matsumura, K.; Endo, M.; Komiyama, M. *J. Chem. Soc., Chem. Commun.* **1994**, 2019. (h) Hovinen, J.; Guzaev, A.; Azhayeva, E.; Azhayev, A.; Lönnberg, H. *J. Org. Chem.* **1995**, 60, 2205.
- Smith, J.; Ariga, K.; Anslyn, E. V. *J. Am. Chem. Soc.* **1993**, 115, 362.
- Gerlt, J. A.; Gassman, P. G. *Biochemistry* **1993**, 32, 11943.
- Branch, G. E. K.; Calvin, M. In *The Theory of Organic Chemistry*; Prentice-Hall, New York, 1941; pp 183–270.
- Kluger, R.; Covitz, F.; Dennis, E.; Williams, D.; Westheimer, F. H. *J. Am. Chem. Soc.* **1969**, 91, 6066.
- Guthrie, J. P. *J. Am. Chem. Soc.* **1977**, 99, 3991.
- McClelland, R. A.; Cramm, D. A.; McGall, G. H. *J. Am. Chem. Soc.* **1986**, 108, 2416.
- Granoth, I.; Martin, J. C. *J. Am. Chem. Soc.* **1979**, 101, 4618.
- Kneeland, D. M.; Kottke, T.; O'Connor, D.; Anslyn, E. V., manuscript in preparation.
- McClelland, R. A.; Seaman, N. E.; Cramm, D. *J. Am. Chem. Soc.* **1984**, 106, 4511.
- (a) Breslow, R.; Xu, R. *Proc. Natl. Acad. Sci. U.S.A.* **1993**, 90, 1201. (b) Herschlag, D. *J. Am. Chem. Soc.* **1994**, 116, 11631, and references in both these articles.
- Anslyn, E.; Breslow, R. *J. Am. Chem. Soc.* **1989**, 111, 8931.
- (a) Cleland, W. W.; Kreevoy, M. M. *Science (Washington, DC)* **1994**, 264, 1887. (b) Cleland, W. W. *Biochemistry* **1992**, 31, 317.

39. Warshel, A.; Papazyan, A.; Kollman, P. A. *Science (Washington, DC)* **1995**, *269*, 102.
40. Fersht, A. *Enzyme Structure and Mechanism*, 2nd Ed.; W.H. Freeman, 1985; Ch. 5.
41. (a) Thompson, J. E.; Raines, R. T. *J. Am. Chem. Soc.* **1994**, *116*, 5467. (b) Ballinger, P.; Long, F. A. *J. Am. Chem. Soc.* **1960**, *82*, 795.
42. (a) Serpersu, E. H.; Hibler, D. W.; Gerlt, J. A.; Mildvan, A. S. *Biochemistry* **1989**, *28*, 1539. (b) Weber, D. J.; Serpersu, E. H.; Shortle, D.; Mildvan, A. S. *Biochemistry* **1990**, *29*, 8632.
43. Jencks, W. P. *J. Am. Chem. Soc.* **1972**, *94*, 4731.
44. For another discussion comparing low-barrier hydrogen bonds and the libido rule see: Gerlt, J. A.; Gassman, P. G. *J. Am. Chem. Soc.* **1993**, *115*, 11552.
45. Iverson, D. J.; Hunter, G.; Blount, J. F.; Damewood Jr., J. R.; Mislow, K. *J. Am. Chem. Soc.* **1981**, *103*, 6073.
46. Metzger, A.; Peschke, W.; Schmidtchen, F. P. *Synthesis* **1995**, 56.
47. Kawasaki, I.; Matsuda, K.; Kaneko, T. *Bull. Chem. Soc. Jpn.* **1971**, *44*, 1986.
48. Kim, E. E.; Wyckoff, H. W. *J. Mol. Biol.* **1991**, *218*, 449.

(Received in U.S.A. 23 September 1996; accepted 18 February 1997)